Proceedings in MANUFACTURING SYSTEMS

Proceedings in Manufacturing Systems, Volume 20, Issue 1, 2025, pp. 17-22 ISSN 2067-9238

INJECTION MOLDING PROCESS IMPROVEMENT BY STRUCTURED SIMULATION EXPERIMENTS: A CASE STUDY

Megan ASENOVA[1] and George-Christopher VOSNIAKOS[2,*],

[1)] MSc graduate student, School of Mechanical Engineering, National Technical University of Athens, Athens, Greece
[2)] Prof., PhD, Manufacturing Technology Laboratory, School of Mechanical Engineering, National Technical University of Athens, Athens, Greece.

Abstract: *Analysis of injection molding of a food packaging container cover through a finite number of simulation runs is presented. Firstly, simulation of the product was set up on Moldex3D™ software, by a 'screening' round of simulation experiments replicating the actual process conditions and matching the process metrics in the injection and packing phases, including the emergence of air traps and the lack of sink marks. In this way, the simulation model was validated. In addition, the degree of influence of each process parameter on the final result was investigated by ANOVA. Based on these insights, Taguchi DoE was implemented on the simulation model aiming at achieving the desired part weight and the minimum clamping force. The best combination of the main process control parameters was obtained highlighting the role of the melt temperature and the Material Flow Index.*

Key words: *injection molding, thin wall; melt temperature, MFI, part weight, clamping force.*

LEGEND

IT : injection time
IP : max injection pressure
PT : packing time
PP : max packing pressure
MFI : material Melt Flow Index
MT : melt temperature
AT : air temperature
PW : part weight
CF : clamping force
CT : cycle time

1. INTRODUCTION

Simulation-based optimization has established itself as a common tool in determining injection-molding process parameters that minimize defects and ensure dimensional and mechanical quality. Early research demonstrated that systematic use of computer-aided engineering (CAE) and response surface methodology can predict and reduce shrinkage and warpage in thin-shell parts [1].

Later developments introduced surrogate models such as Kriging and artificial neural networks, which significantly improved computational efficiency in multi-objective optimization of process conditions [2, 3]. These approaches, coupled with advanced thermoviscoelastic flow simulations, allow reliable prediction of deformation, shrinkage, and warpage while maintaining acceptable cycle times [4, 5].

Accurate modeling of the filling and packing stages has been shown to be critical for achieving complete cavity filling and avoiding defects such as short shots and air traps [6]. Recent studies use CAE-driven optimization to establish balanced pressure and temperature distributions that prevent such issues and enhance overall part quality [7]. Weld lines, which typically reduce mechanical strength and surface aesthetics, are now predicted directly from simulated flow-front convergence; process optimization and localized mold-temperature control have been demonstrated to reduce their visibility and improve structural performance [8].

Cooling design also plays a central role in dimensional stability. The use of conformal cooling channels designed through conjugate heat-transfer simulations has reduced thermal gradients, residual stress, and warpage while shortening the cooling cycle [9–12]. Machine-learning and evolutionary algorithms further improve part uniformity and productivity [13].

Integration of CAE, data-driven models, and digital-twin frameworks enable simultaneous optimization of temperature profiles, injection/packing pressure, and cooling [14]. This provides prediction and adaptation towards defect-free parts that satisfy geometric, surface, and mechanical property specifications [15].

This work presents the workflow as well as implementation details concerning process understanding and subsequently process parameter optimization for injection molding of thin-walled food container caps.

Essentially, this methodology can be applied to any pressure-die cast product. Section 2 reviews literature pertaining to the use of Taguchi DoE and optimization tools in conjunction with injection molding. Section 3 presents the part studies and the simulation tool used. Section 4 outlines the DoE setup and results obtained. Section 5 sums up conclusions and suggests future work.

[*] Corresponding author: Heroon Polytehniou 9, Athens 15773, Greece,
Tel.: +30 210 7721457,
E-mail address: *vosniak@central.ntua.gr* (G.-C. Vosniakos).

2. LITERATURE REVIEW

The use of Taguchi orthogonal designs in conjunction with injection-molding simulation has been increasingly adopted to effectively identify robust process settings while limiting the number of simulation runs. In a typical study [16], a Taguchi L27 array was used with Moldflow simulation to determine optimal levels of melt temperature, coolant (mold) temperature, packing time, packing pressure, and cooling time to minimize warpage and shrinkage in biodegradable polymer blends (e.g., PLA, PLA–TPU). The Taguchi–ANOVA results indicated that melt temperature, coolant temperature, and packing time significantly influenced both shrinkage and warpage.

Further work combines Taguchi design with metaheuristic optimization. For example, Zhang et al. [17] integrated Taguchi design with a particle swarm optimization (PSO) algorithm and Moldflow simulation to minimize warpage in LCD back cover parts. The Taguchi method was used to screen influential parameters and supply initial settings, while PSO refined the solutions, achieving errors under 2.5% relative to simulation predictions. In thin-walled geometries, hybrid methods merging simulation, Taguchi, and neural networks (ANN) have been applied. In a study using finite element simulation and Taguchi L18 design, short-shot volume, shrinkage, and warpage were concurrently optimized [18]. Cooling channel optimization has also been addressed via Taguchi-influenced simulation. Design and fabrication of conformal cooling channels (CCC) was reviewed in [9] including case studies where Taguchi design guided simulation of cooling layouts to reduce warpage and cycle time. Typical warpage and shrinkage optimization via process-parameter tuning, comparing multiple strategies including Taguchi and simulation, surrogate modeling, and multi-objective optimization is presented in [19].

Other simulation-DOE works include studies of conformal cooling channel simulation comparisons [20], thermal/warpage modeling of CCC designs [21], and the application of Taguchi + simulation to commercial molded components to reduce shrinkage and cycle time [22]. Finally, the design of CCC via generative methods linked to simulation is emerging, offering new hybrid workflows for integrating Taguchi-like parameter screening in automated design loops [23].

3. MATERIALS AND METHODS

3.1. The part

The part studied is shown in Figure 1. It is a lid of a dairy products container made of polypropylene (PP) grade J-690K by Borealis™. The mold is designed by company Bazigos™, therefore its geometry is taken for granted. The purpose of the investigation is to optimize the controllable process parameters.

Fig. 1. The part studied of diameter 97.6 mm and weight 4.2 gr.

3.2. The simulation setup

The simulation tool used is Moldex3D™ Studio 2022. The mold is designed focusing on the feeding system. The 'pin type' gate of truncated conical shape (cone diameters: 6 mm and 2 mm, cone length: 6 mm) is adopted to replicate the feeding system already in place. The Moldbase™ wizard constructs a default box-like mold whose cross-section measures 197 × 197 mm. see Fig. 2,*a*. Similarly, the Cooling Channel™ wizard constructs a default cooling system consisting of parallel channels of diameter 8 mm. Two layers, each consisting of 4 parallel channels at a center line distance of 16 mm from each other and a layer center line distance of 24 mm determine the cooling system configuration, Fig. 2,*b*.

The 3D model is automatically meshed with 2,268,390 solid elements for the lid and 1,792 for the hot runner. At the mold-part interface the finest mesh available (level 5) was chosen consisting of 16,810 elements. Mesh healing functionality ensured that the mesh was healthy and appropriate for the numerical simulation that followed.

The material was selected from Moldflow™ library having MFI = 45 g/10 min.

Although transient analysis is usually conducted covering filling, packing and, cooling, in this case only the filling and packing phases were focused on because cooling was handled by the software tool as ideal, i.e. essentially excluded from further analysis.

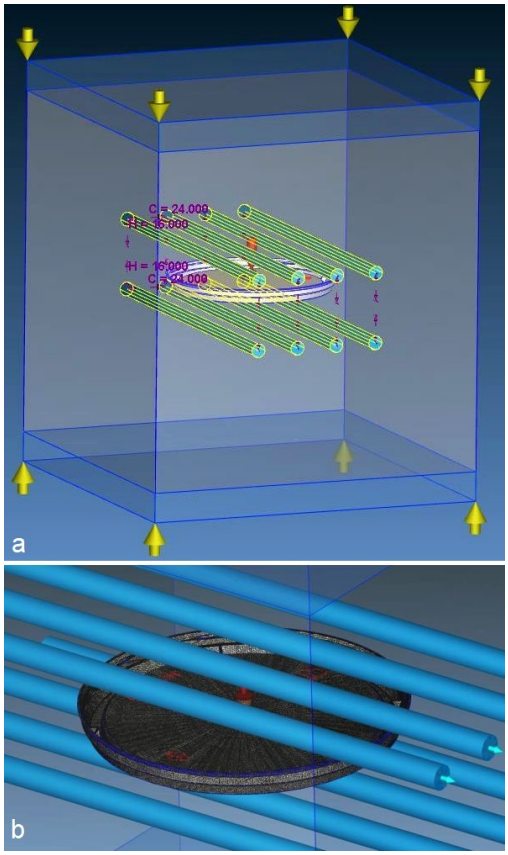

Fig. 2. The mold: *a* – general configuration; *b* – cooling system.

Table 1

Initial process parameters adopted in the simulation

Parameter	Units	Value
Filling time target	s	0.1
Melt temperature	°C	240
Mold temperature	°C	20
Max injection pressure	MPa	160
Injection volume	cm^3	4.76252
Packing time target	s	0.3
Max packing pressure	MPa	70
Cooling time target	s	1.3
Mold open time	s	3.4
Ejection temperature target	°C	90
Air temperature	°C	25
Cycle time target	s	5.1
Hot runner residence time	s	5.18688

The solver engaged was Enhanced-P with 'Customize' option selected to activate compressible, non-Newtonian flow with viscous heating.

3.3. Initial validation of simulation

As a first step, a simulation run was executed with the exact process parameter values used in day-to-day production. These are shown in Table1. The flow velocity and the packing pressure profiles used were taken from the actual setup of the injection molding process. They are shown in Fig. 3.

The filling time resulting from simulation was 0.148 sec and homogenous filling during this time is observed resulting in complete filling of the mold cavity. Air bubble traps were revealed, see Fig. 4,*a*, which was expected therefore air vents had been foreseen to counter this problem. No weld line defects are observed. The maximum value of pressure during the filling stage reached 157 MPa, which is acceptable, given that higher pressure drop is expected in the real feeding system as opposed to the simplified one used in the simulation. At

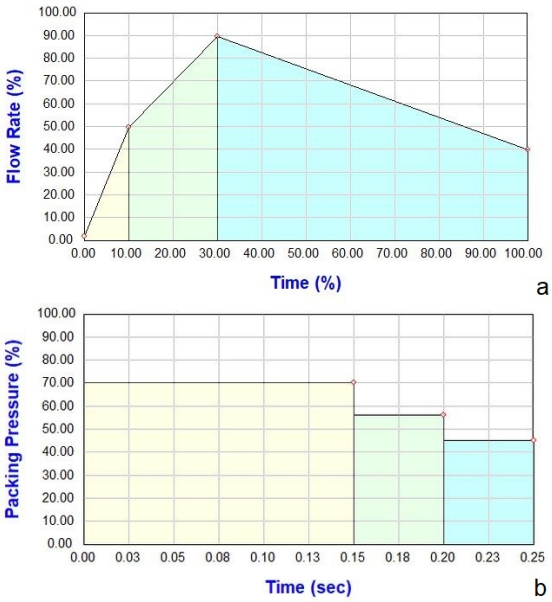

Fig. 3. Injection molding process: *a* – flow rate profile; *b* – packing pressure profile.

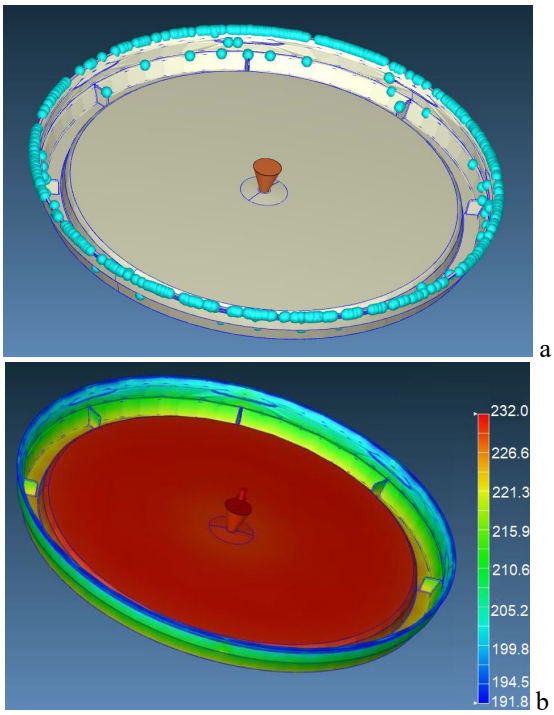

Fig. 4. Results at the end of filling phase (a) Air traps at the rim and ribs (b) temperature distribution.

the end of the filling phase the maximum temperature reached 232 °C, concentrated at the pin gate, as expected. Temperature distribution at the end of this phase is shown in Fig. 4,*b*. Shear stress is low enough (mostly below 1.2 MPa) to justify lack of high residual stresses. The maximum clamping force was observed at the end of the filling phase and was equal to 43 t, exactly when the runner pressure reached its maximum value, too.

Regarding the packing phase, simulation provides valuable insights, too. Packing pressure at the end of this phase is shown in Fig. 5,*a*. In general, overpacking, i.e. excessive pressure, is to be avoided since this may lead to flash building. Melt front time is the sum of filling and packing times, i.e. 0.417 s. Temperature at the end of the packing phase is lower than that at the end of the filling phase given that about 90% of the part has solidified.

Average volumetric shrinkage is 6.6% i.e. above the tolerable limit. However, this is misleading because most of the shrinkage happens during cooling, which is not considered in this case. The frozen layer ratio at the end of packing is on the average 99.16%, just short of the desirable ideal of 100%, see Fig. 5,*b*.

The average index for sink marks is 0.007 (standard deviation: 0.012), pointing to low probability of sink marks emergence. Negative figures imply overpacking, whilst positive figures indicate inadequate packing.

Further, the sprue pressure increases up to 159 MPa at 0.145 s and then falls gradually to zero when the gate solidifies. In addition, the clamping force rises to 48 t at 0.166 sec and falls in a similar manner, see Fig. 6. However, note that for a 45 t press taking a safety margin into account clamping force should be at most 40–42 t. Its reduction can be linked to an increase in melt temperature; in fact, it is observed that clamping force decrease starts at the last stage of packing, i.e. when the temperature of the melt starts decreasing.

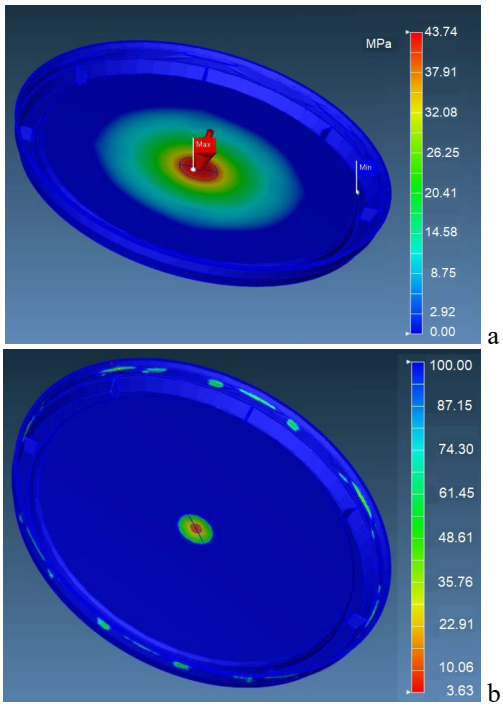

Fig. 5. Results at the end of the packing phase: *a* – pressure distribution; *b* – volumetric shrinkage distribution.

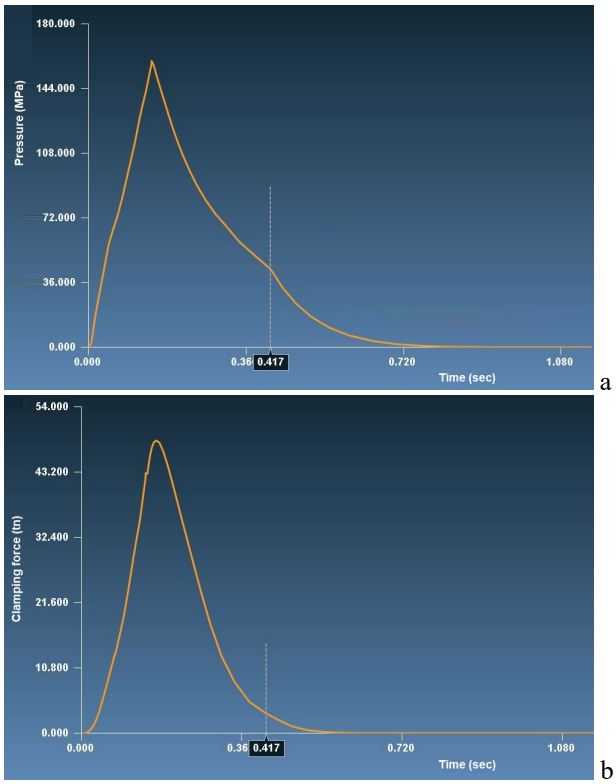

Fig. 6. Evolution of: *a* – packing pressure; *b* – clamping force.

4. TAGUCHI DOE

Given the large number of control parameters, it was decided to do first a screening DoE comprising 7 parameters at 2 extreme levels each to serve as sensitivity analysis. The most important parameters are then examined in a second DoE with more detail. Since cooling was considered ideal, no pertinent parameters were considered in either DoE.

Table 2

Design and results of screening Taguchi DoE

No	Control Factors							Quality factors		
	IT	PT	IP	PP	MT	MFI	AT	PW	CF	CT
	s	s	MPa	MPa	°C	g/ 10 min	°C	g	t	s
1	0.08	0.25	150	50	220	45	5	4.107	49.1	5.03
2	0.08	0.25	150	100	260	100	25	3.980	41.9	5.03
3	0.08	0.40	200	50	220	100	25	3.996	53.1	5.18
4	0.08	0.40	200	100	260	45	5	4.092	32.6	5.18
5	0.15	0.25	200	50	260	45	25	4.086	32.4	5.10
6	0.15	0.25	200	100	220	100	5	4.040	66.0	5,10
7	0.15	0.40	150	50	260	100	5	3.978	39.7	5.25
8	0.15	0.40	150	100	220	45	25	4.154	60.0	5.25

Table 3

Importance of control factors of the screening DoE. Cont: ANOVA % Contribution, S/N: Taguchi Signal-to-Noise ratio, R: Rank

	PW			CF			CT		
	S/N	Cont (%)	R	S/N	Cont (%)	R	S/N	Cont (%)	R
IT	19.91	2.86	4	0.78	5.34	4	0.12	**17.88**	**2**
PT	10.99	0.02	6	0.14	0.19	6	**0.25**	**82.12**	**1**
IP	14.20	0.01	5	0.61	0.51	5	0.00	0.00	3
PP	21.93	4.07	3	10.38	**8.01**	**3**			
MT	31.71	**10.77**	**2**	38.46	**77.70**	**1**			
MFI	74.05	**82.27**	**1**	13.63	**8.26**	**2**			
AT	0.90	0.00	7	0.07	0.00	7			

4.1. Screening DoE

The quality factors investigated concerned the part weight (PW), constituting a major user requirement, the clamping force (CF) pointing to suitability of the press and the cycle time (CT) indicating productivity.

PW follows the 'nominal-the-best' criterion, whereas CF and CT follow the smaller-the-better criterion. Thus, the respective formulae are used for S/N calculation.

The control parameters are: injection and packing time (IT, PT), max injection and packing pressure (IP, PP), material (MFI), melt temperature (MT). Air temperature (AT) is also considered as a noise factor. Table 2 summarizes the DoE and its results.

Signal-to-Noise ratio (S/N) and Analysis of Variance (ANOVA) performed on Excel™ yielded the results shown in Table 3.

According to these results, the material will be fixed to polypropylene with MFI=45 gr/10min as its influence is obvious and does not need further investigation.

Furthermore, air temperature influence is negligible and will be fixed at 25 °C. Thus, injection and packing time (IT, PT) and pressure (IP, PP) are the four control factors to focus on, complemented by melt temperature (MT).

Cycle time (CT) is clearly influenced by IT and PT, but the difference between maximum and minimum values attained is small anyway. Thus, it was dropped in the new DoE. It is noteworthy that in the respective ANOVA the degrees of freedom (DOF) and Sum of squares (Se) of the error terms are zero, so the ratio of deviations *F* cannot be calculated.

4.2. Detailed DoE

The wide range of time factors (IT, PT) adopted in the screening DoE was reduced in the detailed DoE following expert advice by the collaborating company's engineers. Pressure (IP, PP) was deemed more interesting to experiment with, thus adopting three levels for each. Melt temperature had a significant contribution to both PW and CF, hence it was considered interesting to examine three levels for it, too, also given its significant influence on melt viscosity which is fundamental to flow characteristics.

Table 4 summarizes the DoE and its results. S/N and ANOVA yielded the results shown in Table 5.

Figure 7 depicts the main effects diagrams for part weight and for clamping force.

Regarding part weight (PW), the main influencing factor is Melt Temperature. All the rest control factors are reflected in a change of part weight at the third decimal point, i.e. differences are negligible. Regarding clamping force (CF), the main influencing factor is Melt Temperature (MT) even more than in the previous case. PT, PP and IP have negligible influence, whereas IT has some influence; however, the first two levels correspond to a difference of just 2 t of clamping force.

4.3. Control factor optimisation

Based on Fig. 7, the optimal combination of control factors is shown in Table 6. The main factor influencing both PW and CF is MT and fortunately, it has the same optimal value, namely 250 °C. IP and PP do differ for PW and CF respectively, but their levels do not cause that much difference in the result, so they can be neglected. PT has also the same optimal level for both PW and CF. IT has different optimal levels for PW and CF, but as stated before, the respective difference in PW is 2 t.

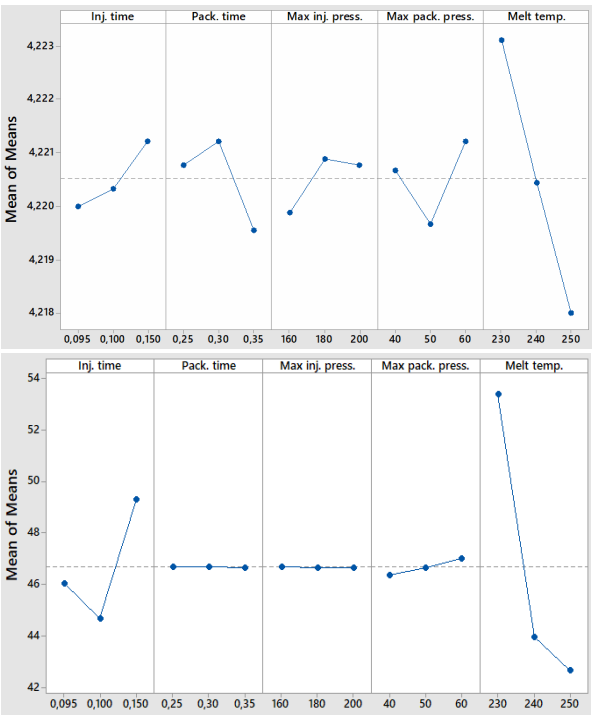

Fig. 7. Taguchi main effects: *a* – part weight; *b* – clamping force.

Table 4

Design and results of the detailed Taguchi DoE

No	Control Factors					Quality factors	
	IP	PP	IT	PT	MT	PW	CF
	MPa	MPa	sec	sec	ºC	gr	tn
1	160	40	0.095	0.25	230	4.223	51.30
2	180	40	0.095	0.30	240	4.220	42.90
3	200	40	0.095	0.35	250	4.218	42.70
4	200	50	0.095	0.30	230	4.222	51.70
5	160	50	0.095	0.35	240	4.219	43.20
6	180	50	0.095	0.25	250	4.217	43.20
7	180	60	0.095	0.35	230	4.222	52.20
8	200	60	0.095	0.25	240	4.220	43.60
9	160	60	0.095	0.30	250	4.219	43.70
10	180	60	0.100	0.35	250	4.220	41.90
11	200	60	0.100	0.25	230	4.221	51.00
12	160	60	0.100	0.30	240	4.221	42.30
13	160	40	0.100	0.25	250	4.219	41.20
14	180	40	0.100	0.30	230	4.222	50.10
15	200	40	0.100	0.35	240	4.219	41.60
16	200	50	0.100	0.30	250	4.220	41.50
17	160	50	0.100	0.35	230	4.221	50.60
18	180	50	0.100	0.25	240	4.220	41.90
19	200	50	0.150	0.30	240	4.222	46.70
20	160	50	0.150	0.35	250	4.210	43.30
21	180	50	0.150	0.25	230	4.226	57.90
22	180	60	0.150	0.35	240	4.222	46.80
23	200	60	0.150	0.25	250	4.220	43.50
24	160	60	0.150	0.30	230	4.226	58.20
25	160	40	0.150	0.25	240	4.221	46.60
26	180	40	0.150	0.30	250	4.219	43.10
27	200	40	0.150	0.35	230	4.225	57.70

Table 5

Importance of control factors of the detailed DoE

	PW			CF		
	S/N δ	Cont (%)	Rank	S/N δ	Cont (%)	Rank
IP	0.6109	2.246	4	0.0093	0.00156	4
PP	0.8729	4.646	3	0.1257	0.26445	3
IT	0.2731	2.985	5	0.8263	13.45277	2
PT	0.9005	5.569	2	0.0054	0.00039	5
MT	2.3028	48.862	1	19.347	81.68961	1

Table 6

Optimal process parameter values from Taguchi DoE

Quality Factors	IP MPa	PP MPa	IT sec	PT sec	MT ºC
PW	160	50	0.095	0.35	250
CF	200	40	0.100	0.35	250
PW & CF	160	50	0.100	0.35	250

Executing the simulation with the optimal process parameter values for PW & CF from Table 6, yielded a part weight of 4.226 g, which is acceptable since it is within the 3% tolerance from the desirable value of 4.2 g stated by the customer. This is to be compared with the part weight values shown in Table 2 (screening DoE) where none of the 8 experiments was within tolerance.

Furthermore, clamping force corresponding to the optimal conditions resulted as 41.2 t, which is reached at 0.117 s. This is again within the desired 40–42 t range, i.e. a reduction of 14% compared to the 48 t value of the

screening DoE, and was achieved 0.049 s earlier (30% reduction).

Optimal conditions resulted in a sprue pressure of 99 MPa reached at 0.097 s, compared to of 159 MPa reached at 0.145 s in the screening DoE, which is a very considerable alleviation of load reached as a side-effect since this was not an optimization criterion. As regards volumetric shrinkage, the average value was reduced from 6.6% to 5.6%, which is still too high; note, however, the remarks made in the screening DoE discussion (Section 3.3) that this figure is connected to ideal cooling, during which most of the shrinkage occurs.

5. CONCLUSIONS AND OUTLOOK

Despite the better results obtained by high MFI, the lower MFI polypropylene (45 g/10 min) was opted for, since the results were still acceptable but its cost was significantly lower than its high MFI counterpart.

Melt temperature had the overwhelmingly largest influence on clamping force and on part weight. The highest temperatures proved beneficial. The rest of the control factors have reduced influence on the results, but only in the range examined. The latter are generally very narrow, as they result from consultation with experts.

The very low ANOVA error values complementing Taguchi DoEs indicate the proper setup of the latter.

Future work involves investigation of the exact cooling system (geometry and flow rate), which was considered as ideal to simplify the analysis. Such extended modelling is necessary primarily to enable realistic estimation of shrinkage and, as a result, residual stresses and warpage at the end of the cooling phase.

Acknowledgments: The company Bazigos S.A. is gratefully acknowledged for providing the case study data as well as guidance on the process parameter ranges worthy of examination.

REFERENCES

[1] K.-T. Chiang, F.-P. Chang. *Analysis of shrinkage and warpage in an injection-molded part with a thin shell feature using the response surface methodology*, Int. J. Adv. Manuf. Techn., 35, 5–6, 2007, 468–479.

[2] Y. Gao, X. Wang. *An effective warpage optimization method in injection molding based on the Kriging mode*, Int. J. Adv. Manuf. Techn., 38, 9–10, 2008, 926–935.

[3] H. Shi, Y. Deng, Y. Liu. *A warpage optimization method for injection molding using artificial neural network with weighted expected improvement*, Int. Polymer Processing, 27, 1, 2012, 59–68.

[4] X. Zhang, F. Xu, L. Xu. *Simulation-based warpage optimization for injection-molded parts using Kriging surrogate modeling*, J. Mat. Proc. Techn., 197, 1–3, 2008, 120–128.

[5] X. Xie, Y. Wang, S. Zhang, J. Li, Q. Chen. *Multiple-objectives optimization of injection-molding process for defects in plastic products*, Sci. Reports, 14, 2024, 102345.

[6] M. Baum, D. Anders, T. Reinicke. *Enhancing injection molding simulation accuracy: Modeling choices and validation strategies*, Appl. Sciences, 14, 18, 2024, 8468.

[7] G. Tosello, H. N. Hansen, M. Calaon. *Simulation of surface roughness and replication in polymer micro-injection molding*, CIRP J. Manuf. Sci. Techn., 41, 2023, 90–102.

[8] S. Liparoti, M. Calaon, M. Sorgato, G. Lucchetta, G. Tosello. *Analysis of weld lines in micro-injection molding*, Micromachines, 14, 8, 2023, 1506.

[9] S. Feng, A. M. Kamat, Y. Pei. Design and fabrication of conformal cooling channels in molds: Review and progress updates, *Int. J. Heat and Mass Transfer*, 171, 2021, 121082

[10] A. Torres-Alba, S. Salcedo-Sanz, Y. Sáez, D. Camacho, J. Del Ser. *A new conformal cooling design procedure for injection molding using evolutionary optimization*, Appl. Sciences, 10, 4, 2020, 1227.

[11] S. A. Jahan, H. El-Mounayri, M. El-Masry. *Optimal conformal cooling channels in 3D-printed dies for plastic injection molding*, Procedia Manuf., 5, 2016, 888–900.

[12] M. S. Shinde, K. M. Ashtankar. *Additive manufacturing–assisted conformal cooling channels in mold manufacturing processes: Review and case studies*, Advances Mech. Engin., 9, 5, 2017, 1–14.

[13] Z. Gao, X. Wang, Y. Ma. *Machine-learning-aided design of conformal cooling channels for injection molds*, J. Intel. Manuf., 34, 9, 2023, 3813–3830.

[14] J. Li, G. Yang, L. Zhang, S. Li. *A predictive modelling strategy for warpage and shrinkage defects in plastic injection molding using fuzzy logic and pattern search optimization*, J. Intel. Manuf., 35, 5, 2024, 2411–2423.

[15] A. Gaspar-Cunha, J. Melo, T. Marques, A. Pontes. A review on injection molding: Conformal cooling channels, modelling, surrogate models and multi-objective optimization, *Polymers*, 17, 7, 2025, 919.

[16] E. Oliaei, B. S. Heidari, S. M. Davachi, A. R. Bahramian, M. R. Saeb. *Warpage and shrinkage optimization of injection-molded plastic spoon parts for biodegradable polymers using Taguchi, ANOVA and artificial neural network methods*, J. Mat. Sci. Techn., 32, 8, 2016, 710–720.

[17] L. Zhang, T.-L. Chang, C.-C. Tsao, K.-C. Hsieh, C.-Y. Hsu. Analysis and optimization of injection molding process on warpage based on Taguchi design and PSO algorithm, *Int. J. Adv. Manuf. Techn.*, 137, 1, 2025, 981-988.

[18] M. Moayyedian, A. Dinc, A. Mamedov. *Optimization of injection-molding process for thin-walled polypropylene part using artificial neural network and Taguchi techniques*. Polymers 13, 23, 2021, 4158.

[19] N. Zhao, J. Lian, P. Wang, Z. Xu. *Recent progress in minimizing the warpage and shrinkage deformations by the optimization of process parameters in plastic injection molding: A review*, Int. J. Adv. Manuf. Techn., 120, 1–2, 2022, 85–101.

[20] O. A. Mohamed, S. H. Masood, A. Saifullah. *A simulation study of conformal cooling channels in plastic injection molding*, Int. J. Engineering Research, 2, 5, 2013, 344–348.

[21] S. Shen, B.B, Kanbur, Y. Zhou & F. Duan. *Thermal and mechanical analysis for conformal cooling channel design in injection molding*, Materials Today: Proceedings, 28, 2020, 396-401.

[22] M. Kariminejad, D. Tormey, S. Huq, J. Morrison, J. Redmond, C. Souto, M. McAfee. *Optimization of a Commercial Injection-Moulded component by using DOE and simulation*, arXiv preprint, 2301, 2023, 11620.

[23] N. Wilson, M. Gupta, M. Patel, M. Mazur, V. Nguyen, S. Gulizia, I. Cole. Generative design of conformal cooling channels for hybrid injection molding tools, *Int. J. Adv. Manuf. Techn.*, 133, 1, 2024, 861-888.